CHAPTER TWO

Analysis of metabolically labeled inositol phosphate messengers by NMR

Robert Puschmann[a,b,†], **Robert K. Harmel**[a,b,†], **Dorothea Fiedler**[a,b,*]
[a]Leibniz-Forschungsinstitut für Molekulare Pharmakologie, Berlin, Germany
[b]Institut für Chemie, Humboldt-Universität zu Berlin, Berlin, Germany
*Corresponding author: e-mail address: fiedler@fmp-berlin.de

Contents

Abstract

Inositol phosphates (InsPs) are an important group of eukaryotic messengers and mediate a wide range of processes. To elucidate the biological functions of these molecules, robust techniques to characterize inositol phosphate metabolism at the cellular level are highly sought after. This chapter provides a detailed protocol for the preparation of ^{13}C-labeled *myo*-inositol, its use for metabolic labeling of mammalian and yeast cells, and the quantitative analysis of intracellular InsP pools from cell extracts using NMR spectroscopy.

† R.P. and R.K.H. contributed equally.

Methods in Enzymology, Volume 641
ISSN 0076-6879
https://doi.org/10.1016/bs.mie.2020.04.035

1. Introduction

1.1 Inositol phosphate signaling molecules

Inositol phosphates are a versatile class of small molecule messengers and are key components in cellular decision-making processes. The inositol phosphates comprise two major groups: the lipid-anchored phosphatidyl inositol phosphates (PtdInsPs), and the soluble inositol phosphates (InsPs) (Balla, 2013; Berridge, 2016; Irvine & Schell, 2001) (Fig. 1). Among the InsPs, the most abundant species in most organisms and cell lines is $InsP_6$ (app. 10–100 μM in mammalian cells) and its high negative charge promotes strong binding to di- and trivalent metal cations, as well as positively charged amino acid side chains (Veiga et al., 2006; Wundenberg & Mayr, 2012). For example, $InsP_6$ was proposed to act as a scaffolding molecule that promotes HIV capsid maturation (Dick et al., 2018; Mallery et al., 2018). Although $InsP_6$ is already densely phosphorylated, inositol-based molecules containing even seven (e.g., 5PP-$InsP_5$/5-$InsP_7$) or eight (e.g., 1,5$(PP)_2$-$InsP_4$/$InsP_8$) phosphate groups exist (Fig. 1). This unique subgroup, termed the inositol pyrophosphates (PP-InsPs), harbors one or two phosphoanhydride bonds and has been investigated more thoroughly in recent years. Genetic perturbation of the kinases that synthesize PP-InsPs (IP6Ks and PPIP5Ks) has linked these molecules to diverse processes, including insulin signaling, tumor cell motility, apoptosis and phosphate homeostasis (Auesukaree, Tochio, Shirakawa, Kaneko, & Harashima, 2005; Bhandari et al., 2007; Chakraborty et al., 2010; Jadav et al., 2016; Koldobskiy et al., 2010; Moritoh et al., 2016; Zhu et al., 2019). Consequently, the enzymes involved in PP-InsP metabolism have become intriguing targets for pharmacological intervention (Wormald, Liao, Kimos, Barrow, & Wei, 2017).

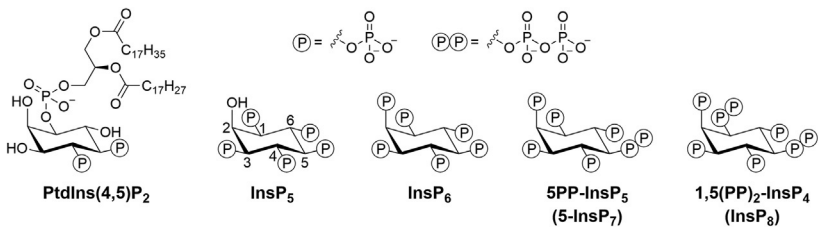

Fig. 1 Examples of inositol phosphate messengers. The numbering of the carbon atoms in the *myo*-inositol ring is indicated in the structure of $InsP_5$.

1.2 Detection and quantification of endogenous inositol phosphates

Genetic studies have established a wide range of functions for InsPs and PP-InsPs in a variety of cellular processes. However, to enable a detailed understanding of the regulation, turnover and dynamic interconversion of these messengers, and to connect specific messengers to defined downstream signaling events, the detection of endogenous InsPs levels remains a crucial task. Due to the absence of UV-active moieties in these molecules, metabolic labeling of cells with radioactive [^{3}H]*myo*-inositol or [^{32}P]orthophosphate has been the most widely used technique in the field (Menniti, Miller, Putney, & Shears, 1993; Stephens et al., 1993). The resulting radioactively labeled InsPs can be isolated by perchloric acid extraction of cell lysates and separated based on their charge using strong anion exchange (SAX) HPLC. Subsequently, collected fractions are analyzed by scintillation counting (Fig. 2A). The incorporation of radioactive labels has contributed to many essential discoveries (Banfic, Bedalov, York, & Visnjic, 2013; Gu et al., 2017; Menniti et al., 1993; Stephens et al., 1993), but the requirement to work with radioactive materials and dedicated equipment, and the limited compatibility with

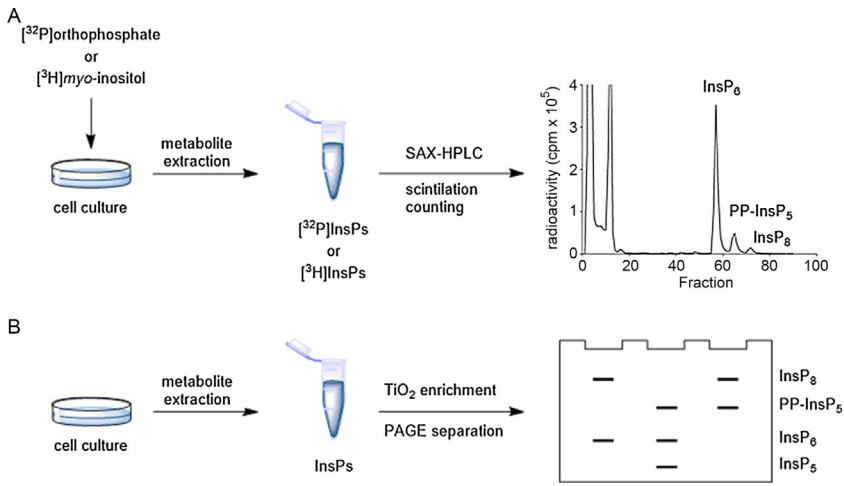

Fig. 2 Analytical techniques to monitor endogenous InsPs and PP-InsPs from cell extracts. (A) Metabolic labeling of cells with radioactive material and analysis of InsPs and PP-InsPs by SAX-HPLC using scintillation counting. (B) Unlabeled InsPs and PP-InsPs are enriched using TiO_2 beads followed by PAGE separation and staining with toluidine blue.

certain mammalian cell lines and tissues imposes limitations on its applicability. In a subsequent approach, radioactive labeling could be circumvented by analyzing HPLC fractions using a metal-dependent dye (Mayr, 1988). Even though this method allowed quantitative analysis of InsPs, the prerequisite for non-standard HPLC equipment prevented its wide use. More recently, an alternative method avoided the use of the rather harsh HPLC conditions for separation (Wilson, Bulley, Pisani, Irvine, & Saiardi, 2015). Here, InsPs and PP-InsPs were enriched from acidified cell extracts by TiO_2 beads, followed by separation via high percentage polyacrylamide gel electrophoresis (PAGE) (Fig. 2B). Unlabeled PP-InsPs and $InsP_6$ were visualized using a cationic dye (toluidine blue or DAPI) and were analyzed quantitatively by gel imaging. This technique became widely appreciated because it omits radioactive tracers and does not require advanced instrumentation. On the other hand, a more elaborate sample preparation is necessary and the detection is limited to only the most highly phosphorylated InsPs (Wilson et al., 2015).

While all methods mentioned above have been instrumental to understand InsP and PP-InsP function, they were only able to discriminate InsPs based on their charge and lack a clear distinction of the structural isomers. Furthermore, the necessity of various separation steps precluded direct measurements in complex environments like cell extracts. Therefore, novel approaches that discriminate InsPs and PP-InsPs based on their structure and that generate reliable information with limited sample preparation were highly needed. To tackle these challenges, we developed a new method to measure InsP and PP-InsP levels using nuclear magnetic resonance (NMR) spectroscopy (Harmel et al., 2019). In this approach, mammalian or yeast cells are metabolically labeled with [$^{13}C_6$] *myo*-inositol and InsP and PP-InsP levels can subsequently be quantified from acidic cell extracts, without further separation steps (Fig. 3). NMR spectroscopy provides structural information with atomic resolution, and the ^{13}C-nuclei enable targeted monitoring of low abundant InsP species within a highly complex sample. In this chapter, a workflow for metabolic labeling of InsPs and PP-InsPs is provided. Specifically, the chemoenzymatic synthesis of [$^{13}C_6$]*myo*-inositol is covered, followed by a detailed protocol describing metabolic labeling of mammalian and yeast cells and the subsequent analysis by NMR spectroscopy.

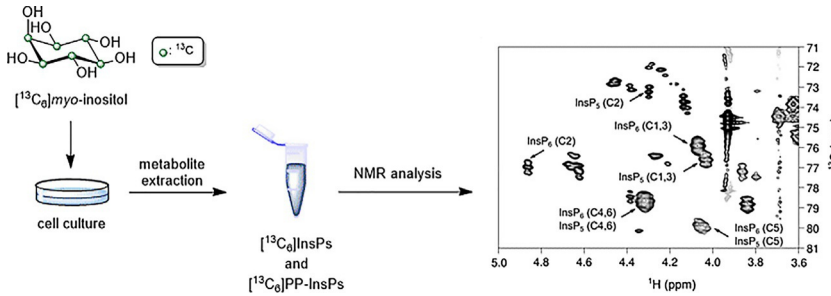

Fig. 3 Metabolic labeling with [^{13}C$_6$]*myo*-inositol and analysis of InsPs and PP-InsPs by NMR spectroscopy.

2. Chemoenzymatic synthesis of [^{13}C$_6$]*myo*-inositol

2.1 General synthetic strategy

[^{13}C$_6$]*myo*-Inositol can be synthesized from [^{13}C$_6$]glucose on a gram scale using a three-step enzymatic synthesis, followed by a chemical purification strategy. (Fig. 4) As a first step, [^{13}C$_6$]glucose is phosphorylated at the 6-position by hexokinase. To assure maximal conversion during this step, an ATP regeneration system consisting of creatine kinase and phosphocreatine is applied. Next, the [^{13}C$_6$]glucose-6-phosphate is isomerized to [^{13}C$_6$]*myo*-inositol-3-phosphate by inositol phosphate synthase. Inositol phosphate synthase is not commercially available but can be obtained in high amounts from *E. coli* (Harmel et al., 2019). Using Mg^{2+} ions as a metal cofactor, in place of commonly used paramagnetic Mn^{2+} ions, the reaction progress can be monitored by ^{13}C NMR spectroscopy. During this step, full conversion of the starting material is crucial for the overall synthetic strategy, as residual [^{13}C$_6$]glucose-6-phosphate would contaminate the final product with [^{13}C$_6$]glucose. Without any [^{13}C$_6$]glucose-6-phosphate remaining, unspecific yet robust and commercially available alkaline phosphatase can be used to dephosphorylate [^{13}C$_6$]*myo*-inositol-3-phosphate to yield [^{13}C$_6$]*myo*-inositol together with a large amount of salt- and buffer-contaminants.

To isolate [^{13}C$_6$]*myo*-inositol from this mixture, the crude material is derivatized with an excess of acetic anhydride in pyridine. The obtained [^{13}C$_6$]*myo*-inositol hexakisacetate can then be purified by normal-phase

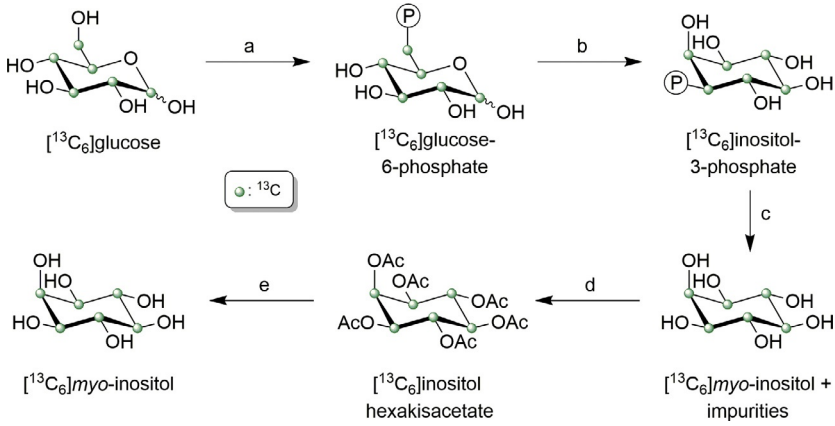

Fig. 4 Chemoenzymatic synthesis of [$^{13}C_6$]myo-inositol followed by derivatization and purification. (A) Hexokinase, creatine kinase, ATP, MOPS pH 6.5, creatine phosphate, DTT, $MgCl_2$, H_2O. (B) Inositol phosphate synthase, NAD^+, Tris pH 8.0, NaCl, $MgCl_2$, H_2O. (C) Alkaline phosphatase, glycine pH 9.8, $ZnCl_2$, H_2O. (D) Ac_2O, pyridine. (E) NaOMe, MeOH.

chromatography. Subsequent saponification and precipitation affords pure [$^{13}C_6$]*myo*-inositol in 55% overall yield (with respect to [$^{13}C_6$]glucose).

2.2 Materials

Enzyme Stock Solutions: Hexokinase (Sigma-Aldrich, H4502): 100 U/mL in 50 mM citrate, pH 7, 10 mM $MgCl_2$, 1 mg/mL BSA. Creatine kinase (Sigma-Aldrich, C3755): 350 U/mL in 200 mM MOPS, pH 6.5, 20 mM $MgCl_2$, 20 mM DTT. Inositol phosphate synthase (Harmel et al., 2019): 4 mg/mL in 20 mM Tris, pH 7.4, 200 mM NaCl, 1 mM DTT. Alkaline phosphatase (Sigma-Aldrich, P5521): 100 U/mL, 10 mM Tris, pH 8.5, 5 mM $MgCl_2$, 0.2 mM $ZnCl_2$, 50% (v/v) glycerol. Hexokinase and creatine kinase stock solutions were kept at −20 °C for several months, multiple freeze-thaw cycles should be avoided. Alkaline phosphatase stock solution was kept at 4 °C for several months.

Chemicals: NaOMe in MeOH, pyridine, MeOH, DCM, creatine phosphate, ATP, NAD^+, glycine, DOWEX® 1 × 8 (Cl^--form), silica TLC plates, NH_4OH, AcOH, NH_4HCO_3, $(NH_4)_2CO_3$, silica gel, hexanes, EtOAc, DOWEX 50WX8 (H^+-form), MeCN, inositol phosphate synthase, D-[$^{13}C_6$]glucose (Eurisotop CLM-1396-10, alternatively, differently labeled glucose can be used as well. [1-$^{13}C_1$]glucose yields [4-$^{13}C_1$] *myo*-inositol, and [4,5-$^{13}C_2$]glucose yields [4-$^{13}C_1$]*myo*-inositol).

2.3 Protocol

Day 1

1. Prepare a solution of D-[$^{13}C_6$]glucose (1.00 g, 83 mM), MOPS (100 mM, pH 6.5), creatine phosphate (87 mM), ATP (1 mM), DTT (20 mM) and $MgCl_2$ (20 mM) in 65 mL (total reaction volume) deionized water.
2. Add hexokinase (1 U/mL) and creatine kinase (1.75 U/mL), mix gently and incubate at 30 °C overnight.

Day 2

3. Test conversion by TLC as explained in related techniques (Section 2.4).
   a. <90% conversion: add more creatine phosphate, hexokinase and creatine kinase and incubate until full conversion is achieved.
   b. >90% conversion: continue with the next step.
4. Prepare anion exchange column:
   Add 50 mL of DOWEX® 1 × 8 (Cl^- form) to a fritted glass column and wash with MeOH (~500 mL) until the eluate becomes colorless, followed by 500 mL deionized water. Equilibrate the column with 300 mL 1 M NH_4HCO_3 and wash with deionized water until the eluate reaches a pH < 8.
5. Dilute the reaction mixture with 320 mL deionized water and load it onto the column. Discard the flowthrough.
6. Wash the column with 300 mL deionized water to remove unreacted [$^{13}C_6$]glucose. Discard the flowthrough.
7. Elute [$^{13}C_6$]glucose-6-phosphate with 250–500 mL of 0.1 M $(NH_4)_2CO_3$ and lyophilize the combined eluates in a round-bottom flask overnight.

Day 3

8. Dissolve the lyophilized solids in 50 mL deionized water.
9. Start reaction by mixing dissolved solids, Tris (50 mM, pH 8.0), NAD^+ (0.5 mM), NaCl (50 mM), $MgCl_2$ (2 mM) and inositol-3-phosphate synthase (40 μg/mL) in 200 mL (total volume) deionized water and incubate at 85 °C for 4 h.
10. Combine 450 μL of the reaction mixture and 50 μL of D_2O into an NMR tube and control conversion by ^{13}C NMR spectroscopy. (Follow disappearance of the doublets at 92 and 96 ppm)
    a. incomplete conversion: add more IPS and incubate until full conversion is achieved.
    b. complete conversion: continue with the next step.

11. Cool the reaction mixture down to 35 °C.
12. Add 15 mL of 1 M glycine pH 9.8, 75 µL of 1 M $ZnCl_2$, fill up to 300 mL with deionized water and adjust the pH to 9.8.
13. Add 1.5 mL alkaline phosphatase stock solution and incubate overnight at 35 °C.

Day 4

14. Test conversion by TLC as explained in related techniques (Section 2.4).
    a. <90% conversion: add more alkaline phosphatase and incubate until full conversion is achieved.
    b. >90% conversion: continue with next step.
15. Concentrate the reaction solution in a 500 mL round-bottom flask to dryness using a rotary evaporator. Coevaporate with 30 mL pyridine and resuspend the crude material in 160 mL pyridine and 70 mL acetic anhydride.
16. Stir the solution under reflux overnight.

Day 5

17. Remove the pyridine by evaporation and re-dissolve the crude material in 500 mL DCM. Add 200 mL of 1 M HCl and pass the suspension through a glass filter.
18. Pour the filtrate into a separatory funnel and separate the organic phase and aqueous phase. (Note: Phase separation is hard to see because of the black solution, so use a flash light to find the separation layer.)
19. Extract the aqueous phase twice with 100 mL DCM and discard the aqueous phase. Wash the combined organic phases with 1 M $NaHCO_3$, then brine.
20. Dry the organic phase with Na_2SO_4 and remove the solids by filtration.
21. Add Telos® 50–100 mL to the filtrate and remove the DCM by rotary evaporation.
22. Purify the immobilized product on a normal-phase silica column (8 × 20 cm) using a step-wise gradient elution (hexane:EtOAc, 10:1 → 5:1 → 1:1 → 1:2; 1.5 L per step).
23. Analyze fractions by LC-MS (look for the Na adduct, m/z 461). Combine and evaporate all fractions that contain product.
24. Analyze the product by NMR spectroscopy and HRMS: **^{1}H NMR** (600 MHz, $CDCl_3$) δ 5.79–5.54 (m, 1.5H), 5.53–5.32 (m, 1.5H), 5.32–5.12 (m, 1.5H), 5.11–4.82 (m, 1.5H), 2.20 (s, 3H), 2.01 (s, 3H), 2.01 (s, 6H), 2.00 (s, 6H). **^{13}C NMR** (151 MHz, $CDCl_3$) δ

169.94 (s), 169.81 (s), 169.56 (s), 71.68–70.65 (m), 70.11–69.15 (m), 69.11–67.90 (m), 20.89 (s), 20.69 (s), 20.60 (s). **HRMS** (ESI/Orbitrap) m/z: $[M+K]^+$ calcd. For $C_{12}^{13}C_6H_{24}KO_{12}$ 477.1101; Found 477.1091.

Day 6

25. Dissolve [$^{13}C_6$]*myo*-inositol hexakisacetate (1.20 g, 2.7 mmol) in methanol (249 mL) and add 5.4 M NaOMe in MeOH (3.35 mL, 18.1 mmol). Stir for 2 h.

26. Neutralize the resulting suspension by addition of DOWEX 50WX8 (H^+ form).

27. Pass the suspension through a glass filter and wash the residue with methanol (100 mL) and water (100 mL) to dissolve all precipitates. Concentrate the filtrate to dryness with a rotary evaporator.

28. *Re*-dissolve the solids using minimal amount of water and precipitate the [$^{13}C_6$]*myo*-inositol by addition of a large excess of cold MeCN.

29. Collect the white precipitate with a glass filter, wash the residue with cold MeCN and re-dissolve in water. Lyophilize [$^{13}C_6$]*myo*-inositol overnight.

Day 7

30. Analyze the product by NMR spectroscopy and HRMS: **^{1}H NMR** (600 MHz, D_2O, pD 7.0) δ 4.29–4.14 (m, 0.5H), 4.03–3.90 (m, 0.5H), 3.82–3.60 (m, 2H), 3.59–3.34 (m, 2.5H), 3.25–3.12 (m, 0.5H). **^{13}C NMR** (151 MHz, D_2O, pD 7.0) δ 74.96–73.80 (m), 72.86–71.71 (m), 71.60–70.50 (m). **HRMS** (ESI/Orbitrap) m/z: $[M-H]^-$ calcd for $^{13}C_6H_{11}O_6$ 185.0762; Found 185.0814.

31. Prepare 50 mM stock solutions in milli-Q water for metabolic labeling experiments.

2.4 Related techniques

Thin layer chromatography (TLC)

1. Spot a drop of the reaction mixture on a silica normal-phase TLC plate.

2. Spot reference compounds (glucose, glucose-6-phosphate, inositol) on the TLC plate.

3. Dry TLC plate gently with a heat gun or under vacuum.

4. Run the TLC plate with MeOH:H_2O:NH_4OH:AcOH, 50:30:15:5 until the solvent front is close to the top of the TLC plate.

5. Dry the TLC with a heat gun and heat until yellow/brown dots appear (for glucose and glucose-6-phosphate) or stain the plate with $KMnO_4$ (for inositol).

3. Metabolic labeling

3.1 General approach

Metabolic labeling with [$^{13}C_6$]*myo*-inositol is conducted analogously to labeling with [^{3}H]*myo*-inositol (Azevedo & Saiardi, 2006). Both approaches are applicable to cell lines that are able to import exogenous *myo*-inositol, and importantly [$^{13}C_6$]*myo*-inositol is non-toxic. The cells of interest are grown in synthetic medium that is devoid of regular ^{12}C-*myo*-inositol and instead supplemented with [$^{13}C_6$]*myo*-inositol. Steady state labeling is usually achieved after at least seven doublings. The labeled cells are subsequently harvested and the inositol phosphates are extracted using perchloric acid. In our hands, the PP-InsPs are stable during this procedure despite the low pH, as long as all solutions are kept on ice and the samples are processed in a timely manner. The acidic extracts are neutralized with KOH to assure pH stability during the following lyophilization step. Although significant amounts of $KClO_4$ precipitate out of solution during the neutralization, it is important to reduce the salt concentration further to enable high quality NMR measurements. Therefore, the lyophilized residue is resuspended in a small volume of D_2O and incubated on ice to lower the salt content as much as possible.

Depending on the biological question to be addressed, different types of NMR measurements can be employed. Only a small spectral window to cover the InsP and PP-InsP resonances is defined (spectral width in the indirect dimension(F1): 40 ppm), when the focus lies exclusively on the highly phosphorylated inositols. In an initial measurement, a high number of points in the F1 dimension (number of FIDs: 512) with a low number of scans (number of scans: 40) should be recorded to observe splitting of the ^{13}C-nuclei. The triplet pattern is characteristic for peaks that correspond to [$^{13}C_6$]*myo*-inositol derived compounds. Once the characteristic peaks are assigned, their signal intensities can be increased in a second measurement with lower resolution (number of FIDs: 128) and a higher number of scans (number of scans: >160) (for representative spectra see Fig. 5).

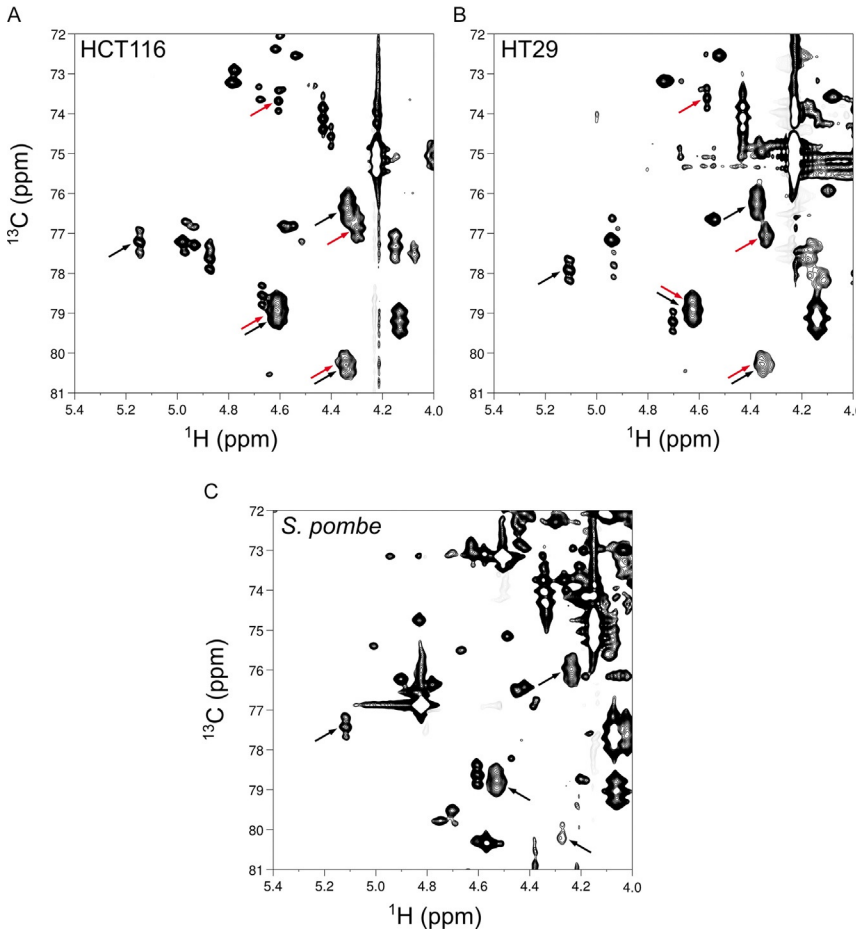

Fig. 5 NMR-spectra of extracts from (A) HCT116, (B) HT29, and (C) *S. pombe*. The spectra were recorded at 310 K and pH* 6.0. The red and black arrows indicate the $InsP_5$ and $InsP_6$ peaks, respectively.

In order to unambiguously assign the observed peaks to a certain InsP species, a synthetic standard should be used as a reference (for synthesis of the different standards please refer to (Puschmann, Harmel, & Fiedler, 2019)). For preliminary assignments, a table of characteristic chemical shifts is included in this protocol (Table 1). In case the InsPs and PP-InsPs signals are obstructed by other, high-intensity peaks, a TiO_2 enrichment can simplify the spectrum by retaining only InsPs and PP-InsPs in the sample (Wilson et al., 2015).

Table 1 Reference peaks for *myo*-inositol, $InsP_5$, $InsP_6$, and PP-$InsP_5$.

Compound	H1/C1	H2/C2	H3/C3	H4/C4	H5/C5	H6/C6
myo-inositol	3.70/74.0	4.23/75.1	3.70/74.0	3.79/75.3	3.45/77.3	3.79/75.3
$InsP_5$	4.34/77.1	4.57/73.6	4.34/77.1	4.62/78.9	4.35/80.3	4.62/78.9
$InsP_6$	4.37/76.2	5.11/72.9	4.37/76.2	4.62/78.9	4.35/80.3	4.62/78.9
5PP-$InsP_5$	4.23/75.1	5.07/78.1	4.23/75.1	4.69/78.9	4.45/80.3	4.69/78.9

The chemical shifts are given as ^{1}H (ppm)/^{13}C (ppm) at 310 K and pH* 6.0.

NMR spectroscopy is a quantitative method and the spectra can be used to determine the absolute concentration of the compounds (with respect to packed cell volume). The peaks of the C2-position of *myo*-inositol, $InsP_5$, $InsP_6$, 1PP-$InsP_5$, 5PP-$InsP_5$ and 1,5$(PP)_2$-$InsP_4$ are distinctive and can be used for quantification of these compounds, relative to an internal standard (tetramethyl phosphonium bromide). The ratio of the signal intensities of the internal standard and the C2-positions can be used for quantification, when referenced to a corresponding calibration curve (for each compound an individual curve is required (Harmel et al., 2019)).

3.2 Materials

Cell Culture: [$^{13}C_6$]*myo*-inositol (see Section 2.3), DPBS (gibco 14190-094), TrypLE express (gibco 12605-010), 100 × glutamine (gibco 25030-024), Pen-Strep (gibco 15140-122), cell culture dish 150 mm × 25 mm (corning 430599), vacuum filtration unit 0.2 μm, FBS dialyzed (Gibco 26400-044), PCV Packed Cell Volume Tube (TPP 87005), DMEM (gibco custom formulation of DMEM powder without glucose, without *myo*-inositol, without glutamine, without serine, without sodium bicarbonate, without sodium phosphate, without pyruvate. All missing components, plus 10 mM HEPES, were added back in, substituting 50 μM [$^{13}C_6$]*myo*-inositol for regular *myo*-inositol and the pH was adjusted to 7.4. The medium was sterile-filtered).

Sample preparation: D_2O (Deutero 00506), D_2O ampule (Eurisotop D215T), 5 mm NMR tubes (Deutero Boro500-5-7).

NMR Spectrometer: Bruker Avance III NMR spectrometer (^{1}H-frequency: 600.13 MHz), cryogenically cooled 5 mm QCI-triple resonance probe equipped with a one-axis self-shielded gradient, TopSpin Acquisition Version 3.5-pl6.

3.3 Protocol

1. Grow the mammalian cell line of choice up to 80–90% confluency in a 15 cm dish in DMEM (+ 50 μM *myo*-inositol (unlabeled), 10% DFBS, + 1 × Pen-Strep, + 1 × Gln) and subsequently dilute the cells 1:10 in a 15 cm dish in DMEM (+50 μM [$^{13}C_6$]*myo*-inositol, +10% DFBS, +1 × Pen-Strep, +1 × Gln). Note: cells in medium containing DFBS grow slower than when supplemented with regular FBS.
2. Split the cells at 80–90% confluency with a 1:10 dilution and distribute them in the appropriate number of 15 cm dishes. Depending on the InsP and PP-InsP concentrations in the cell line of interest, up to 10 dishes might be necessary to allow for reliable quantification. Continue the growth in DMEM (+50 μM [$^{13}C_6$]*myo*-inositol, +10% DFBS, +1 × Pen-Strep, +1 × Gln).
3. Once the cells reach 80–90% confluency, they are washed with DPBS and trypsinized. Combine the cells, wash with DPBS, and determine the packed cell volume of the cell suspension (this is only required if cellular concentrations of InsPs and PP-InsPs will be measured). At this point, the cell number can be determined as well.
4. *Steps 4 through 7 are performed at 4°C!* Centrifuge the cell suspension and lyse the cell pellet by adding 5 mL lysis solution (1 M $HClO_4$, 6 mM EDTA). Vortex the suspension repeatedly over the course of 5 min and centrifuge at 20,000 *g* for 10 min to remove all cell debris.
5. Transfer the supernatant into a fresh tube and adjust the pH of the solution to 6.0 by adding 2 M KOH (in our hands KOH is superior to K_2CO_3 as the pH of the solution is more stable during lyophilization). Incubate the neutralized solution on ice for half an hour to ensure precipitation of as much $KClO_4$ as possible, and centrifuge the solution. Transfer the supernatant into a fresh tube and lyophilize the sample.
6. The next day, dissolve the sample in 600 μL D_2O and incubate on ice for 30 min to allow more $KClO_4$ to precipitate. This step is crucial, as a high ionic strength is problematic for the NMR measurements. Remove the precipitate by centrifugation.
7. Optional step: This step is only necessary if weaker signals close to the HDO solvent peak need to be observed. Lyophilize the supernatant and dissolve the residue in 600 μL D_2O from an ampule.
8. Transfer the solution into an NMR tube and record an NMR spectrum (Fig. 5, Table 1) at 310 K: HMQC with a BIRD pulse for suppression of signals from protons not bound to 13C nuclei. The spectra are recorded

using 1024 points, a spectral width of 10,000 Hz (~ 16.7 ppm) and a center of the spectrum at 4.7 ppm in the F2 dimension. In the F2 dimension spectra are recorded as follows:

- For an overview spectrum: 128 points, a spectral width of 15,000 Hz (~100 ppm), a center of the spectrum at 48 ppm and 20 scans.
- For high resolution in the inositol region: 256 points, a spectral width of 6000 Hz (~40 ppm), a center of the spectrum at 70 ppm and 40 scans.
- For higher sensitivity in the inositol region: 64 points, a spectral width of 6000 Hz (~40 ppm), a center of the spectrum at 70 ppm and 200 scans.

3.4 Related techniques

Labeling of Schizosaccharomyces pombe

Bead beater (Precellys Evolution), glass beads.

Prepare a 50 × salt stock (52.5 mg/mL $MgCl_2 \times 6\ H_2O$, 0.735 mg/mL $CaCl_2 \times 2\ H_2O$, 50 mg/mL KCl, 2 mg/mL Na_2SO_4) and a 20 × glucose stock (400 mg/mL glucose). Sterilize by autoclaving and store at 4 °C.

Prepare a 1000 × vitamin stock (w/o *myo*-inositol) (1 mg/mL sodium pantothenic acid, 10 mg/mL nicotinic acid, 10 mg/mL biotin), a 10,000 × mineral stock (5 mg/mL H_3BO_3, 4 mg/mL $MnSO_4$, 4 mg/mL $ZnSO_4 \times 7\ H_2O$, 2 mg/mL $FeCl_3 \times 6\ H_2O$, 0.4 mg/mL MoO_3, 1 mg/mL KI, 0.4 mg/mL $CuSO_4 \times 5\ H_2O$, 10 mg/mL citric acid), a 100 × amino acid stock (7.5 mg/mL lysine·HCl, 7.5 mg/mL arginine·HCl, 7.5 mg/mL leucine), a 100 × histidine (7.5 mg/mL histidine), a 500 × [$^{13}C_6$]*myo*-inositol stock (9.3 mg/mL [$^{13}C_6$]*myo*-inositol), a 25 × uracil stock (1.875 mg/mL uracil), and a 10 × adenine stock (0.75 mg/mL adenine). Sterilize by filtration and store at 4 °C.

Minimal medium (MM; for 1 L): 2.2 mg/mL Na_2HPO_4, 3 mg/mL potassium phthalate monobasic, 1 mg/mL glutamic acid, 20 mL 50 × salt stock, 100 µL 10,000 × mineral stock, 767 mL milliQ water. Mix, autoclave and store at 4 °C. Add 100 mL 10 × adenine stock (depends on nutritional marker), 40 mL 25 × uracil stock (depends on nutritional marker), 50 mL 20 × glucose stock, 10 mL 100 × histidine stock (depends on nutritional marker), 1 mL 1000 × vitamin stock, 10 mL amino acid stock, 2 mL [$^{13}C_6$]*myo*-inositol or [$^{12}C_6$]*myo*-inositol.

1. Pick an individual colony of *S. pombe* from an agar plate and inoculate into 50 mL MM + [$^{13}C_6$]*myo*-inositol and grow for 2 days (or until OD > 7).

2. Use the prepared culture to inoculate in 2 L MM + [$^{13}C_6$]*myo*-inositol at OD 0.05 and grow the culture overnight until it reaches OD 1.4.
3. Harvest the cells by centrifugation at 4 °C and wash them with ice cold water. Combine all pellets into one tube.
4. Resuspend the cells in a small volume of ice cold water and determine the optical density (OD_{600}).
5. Aliquot 100 ODs of cells into 1.5 mL screw cap tubes and centrifuge.
6. Resuspended the pellet in 600 µL 1 M $HClO_4$, 3 mM EDTA and add glass beads to the meniscus of the suspension. Lyse the cells by bead beating (2 × 20 s, 6500 rpm, 1 min rest on ice in-between cycles).
7. Pierce the bottom of the tubes and collect the cell extract by shortly centrifuging into another tube (30 s, 500 *g*). The debris and the precipitated protein is separated by centrifugation at 20,000 × *g* for 30 min at 4 °C.
8. Continue with Section 3.3, step 5.

TiO_2-enrichment

TiO_2 beads (GL Sciences Inc. 5020-75000), 1 M $HClO_4$, 10% NH_4OH

1. Wash and equilibrate the TiO_2 beads (5 mg per 15 cm dish) with 500 µL water followed by 500 µL 1 M $HClO_4$ (centrifuge for 1 min at 3500 *g*).
2. Add the acidic supernatant from Section 3.3 step 4 to the beads, briefly vortex and rotate the samples for 15 min at 4 °C. If the sample is already neutralized, mix it in a 1:1 ratio with 1 M $HClO_4$.
3. Pellet the beads by centrifugation (1 min, 3500 g) and wash them with 500 µL ice cold 1 M $HClO_4$. Briefly vortex and repeat the wash. The supernatant can be kept to check if all inositol pyrophosphates were removed.
4. To elute, add 250 µL 10% NH_4OH to the pelleted beads, vortex and rotate for 5 min at 4 °C. Pellet the beads and transfer the supernatant (contains the InsPs) to a new tube. Repeat the elution and combine the supernatants to ensure full recovery.
5. Filter the combined eluates through a syringe filter to ensure complete removal of the TiO_2 beads and lyophilize the sample (we recommend lyophilization but alternatively, vacuum concentration using a speed-vac can be implemented).
6. Dissolve the residue in D_2O and check the pH*. Adjust with DCl or NaOD to pH* 6.0 as necessary.

4. Conclusion

The analysis and quantification of InsPs and PP-InsPs in complex samples constitutes a challenging task, since these molecules lack a handle that would facilitate their detection. Most commonly, researchers rely on specific separation techniques, radiolabeling methods, or both, to be able to distinguish and quantify the structurally closely related InsPs and PP-InsPs. Here, we provide a detailed workflow for an alternative approach, in which metabolic labeling of cells with [$^{13}C_6$]*myo*-inositol is followed by NMR analysis. In analogy to previous radiolabeling experiments, eukaryotic cell are exposed to [$^{13}C_6$]*myo*-inositol, but the benign ^{13}C-labeled compound does not require specialized equipment for handling radioactive materials, nor is cell viability affected negatively. The cell extracts are analyzed directly by NMR spectroscopy, and cellular InsPs and PP-InsPs can be quantified within these complex mixtures. In addition to providing information on common InsP species, the labeling strategy with [$^{13}C_6$]*myo*-inositol has also the potential to identify hitherto uncharacterized *myo*-inositol derived metabolites (Harmel et al., 2019). As more research groups will utilize the method described here in a variety of cell lines and organisms, we are certain to uncover novel components and regulatory factors in inositol metabolism.

Acknowledgments

The authors thank Dr. Peter Schmieder for his support with NMR measurements and analysis.

Funding

R.K.H. and R.P. gratefully acknowledge funding from the Leibniz-Gemeinschaft (SAW-2017-FMP-1).

References

Auesukaree, C., Tochio, H., Shirakawa, M., Kaneko, Y., & Harashima, S. (2005). Plc1p, Arg82p, and Kcs1p, enzymes involved in inositol pyrophosphate synthesis, are essential for phosphate regulation and polyphosphate accumulation in *Saccharomyces cerevisiae*. *The Journal of Biological Chemistry*, *280*, 25127–25133.

Azevedo, C., & Saiardi, A. (2006). Extraction and analysis of soluble inositol polyphosphates from yeast. *Nature Protocols*, *1*, 2416–2422.

Balla, T. (2013). Phosphoinositides: Tiny lipids with giant impact on cell regulation. *Physiological Reviews*, *93*, 1019–1137.

Banfic, H., Bedalov, A., York, J. D., & Visnjic, D. (2013). Inositol pyrophosphates modulate S phase progression after pheromone-induced arrest in saccharomyces cerevisiae. *The Journal of Biological Chemistry*, *288*, 1717–1725.

Berridge, M. J. (2016). The inositol trisphosphate/calcium signaling pathway in health and disease. *Physiological Reviews*, *96*, 1261–1296.

Bhandari, R., Saiardi, A., Ahmadibeni, Y., Snowman, A. M., Resnick, A. C., Kristiansen, T. Z., et al. (2007). Protein pyrophosphorylation by inositol pyrophosphates is a posttranslational event. *Proceedings of the National Academy of Sciences of the United States of America*, *104*, 15305–15310.

Chakraborty, A., Koldobskiy, M. A., Bello, N. T., Maxwell, M., Potter, J. J., Juluri, K. R., et al. (2010). Inositol pyrophosphates inhibit akt signaling, thereby regulating insulin sensitivity and weight gain. *Cell*, *143*, 897–910.

Dick, R. A., Zadrozny, K. K., Xu, C., Schur, F. K. M., Lyddon, T. D., Ricana, C. L., et al. (2018). Inositol phosphates are assembly co-factors for HIV-1. *Nature*, *560*, 509–512.

Gu, C., Nguyen, H.-N., Hofer, A., Jessen, H. J., Dai, X., Wang, H., et al. (2017). The significance of the bifunctional kinase/phosphatase activities of diphosphoinositol pentakisphosphate kinases (PPIP5Ks) for coupling inositol pyrophosphate cell signaling to cellular phosphate homeostasis. *The Journal of Biological Chemistry*, *292*, 4544–4555.

Harmel, R. K., Puschmann, R., Nguyen Trung, M., Saiardi, A., Schmieder, P., & Fiedler, D. (2019). Harnessing 13 C-labeled myo -inositol to interrogate inositol phosphate messengers by NMR. *Chemical Science*, *10*, 5267–5274.

Irvine, R. F., & Schell, M. J. (2001). Back in the water: The return of the inositol phosphates. *Nature Reviews. Molecular Cell Biology*, *2*, 327–338.

Jadav, R. S., Kumar, D., Buwa, N., Ganguli, S., Thampatty, S. R., Balasubramanian, N., et al. (2016). Deletion of inositol hexakisphosphate kinase 1 (IP6K1) reduces cell migration and invasion, conferring protection from aerodigestive tract carcinoma in mice. *Cellular Signalling*, *28*, 1124–1136.

Koldobskiy, M. A., Chakraborty, A., Werner, J. K., Snowman, A. M., Juluri, K. R., Vandiver, M. S., et al. (2010). p53-mediated apoptosis requires inositol hexakisphosphate kinase-2. *Proceedings of the National Academy of Sciences of the United States of America*, *107*, 20947–20951.

Mallery, D. L., Márquez, C. L., McEwan, W. A., Dickson, C. F., Jacques, D. A., Anandapadamanaban, M., et al. (2018). IP6 is an HIV pocket factor that prevents capsid collapse and promotes DNA synthesis. *eLife*, *7*, e35335.

Mayr, G. W. (1988). A novel metal-dye detection system permits picomolar-range h.p.l.c. analysis of inositol polyphosphates from non-radioactively labelled cell or tissue specimens. *The Biochemical Journal*, *254*, 585–591.

Menniti, F. S., Miller, R. N., Putney, J. W., Jr., & Shears, S. B. (1993). Turnover of inositol polyphosphate pyrophosphates in pancreatoma cells. *The Journal of Biological Chemistry*, *268*, 3850–3856.

Moritoh, Y., Oka, M., Yasuhara, Y., Hozumi, H., Iwachidow, K., Fuse, H., et al. (2016). Inositol hexakisphosphate kinase 3 regulates metabolism and lifespan in mice. *Scientific Reports*, *6*, 32072.

Puschmann, R., Harmel, R. K., & Fiedler, D. (2019). Scalable chemoenzymatic synthesis of inositol pyrophosphates. *Biochemistry*, *58*, 3927–3932.

Stephens, L., Radenberg, T., Thiel, U., Vogel, G., Khoo, K. H., Dell, A., et al. (1993). The detection, purification, structural characterization, and metabolism of diphosphoinositol pentakisphosphate(s) and bisdiphosphoinositol tetrakisphosphate(s). *The Journal of Biological Chemistry*, *268*, 4009–4015.

Veiga, N., Torres, J., Dominguez, S., Mederos, A., Irvine, R. F., Diaz, A., et al. (2006). The behaviour of myo-inositol hexakisphosphate in the presence of magnesium(II) and calcium(II): Protein-free soluble InsP6 is limited to 49 micro M under cytosolic/nuclear conditions. *Journal of Inorganic Biochemistry*, *100*, 1800–1810.

Wilson, M. S. C., Bulley, S. J., Pisani, F., Irvine, R. F., & Saiardi, A. (2015). A novel method for the purification of inositol phosphates from biological samples reveals that no phytate is present in human plasma or urine. *Open Biology*, *5*, 150014.

Wormald, M., Liao, G., Kimos, M., Barrow, J., & Wei, H. (2017). Development of a homogenous high-throughput assay for inositol hexakisphosphate kinase 1 activity. *PLoS One*, *12*, e0188852.

Wundenberg, T., & Mayr, G. W. (2012). Synthesis and biological actions of diphosphoinositol phosphates (inositol pyrophosphates), regulators of cell homeostasis. *Biological Chemistry*, *393*, 979–998.

Zhu, J., Lau, K., Harmel, R. K., Puschmann, R., Broger, L., Dutta, A. K., et al. (2019). Two bifunctional inositol pyrophosphate kinases/phosphatases control plant phosphate homeostasis. *Elife*, *8*, e43582.